INTERNATIONAL JOURNAL FOR NUMERICAL METHODS IN FLUIDS
Int. J. Numer. Meth. Fluids 2001; **37**: 361–374 (DOI: 10.1002/fld.178)

Response of plane viscous jet to entrance flow rate perturbation

Mohamed Ali Knani[a,1], Taieb Lili[a,2] and Henri-Claude Boisson[b,*,3]

[a] *Laboratoire de Mécanique des Fluides, Faculté des Sciences de Tunis, Université de Tunis II, Tunisia*
[b] *Institut de Mécanique des Fluides de Toulouse, Toulouse, France*

SUMMARY

A two-dimensional numerical simulation solving unsteady incompressible Navier–Stokes equations is used to study the natural varicose instability of a plane jet in the Reynolds number range of 100–900. A transient train of vortices is observed at the beginning of the computation. It disappears yielding a steady flow. This flow is then used at the basis for forced excitation in order to study the space time development of instability. A Reynolds number dependant behaviour is observed which implies that viscosity directly affects the vortex dynamics. Copyright © 2001 John Wiley & Sons, Ltd.

KEY WORDS: excitation; finite volume; instability; numerical simulation; plane jet; unsteadiness; velocity field; vortex

1. INTRODUCTION

The near-field of a plane jet has been long studied in many respects and the Kelvin–Helmholtz instability of the initial shear layer has been found as a key mechanism for the development of the jet. Most of the work concerned reasonably high Reynolds numbers providing a basis for an essentially inviscid development of the vortices (Meyer *et al.* [1], Hussain and Thompson [2], Thomas and Goldschmidt [3]).

However, one of the first works on the domain conducted by Sato [4] concerned low-Reynolds number jets and a theoretical study by Tatsumi and Kakutani [5] was conducted on the basis of a laminar jet profile. This paper aims to study some moderate Reynolds number flows in which the viscous effect is likely to affect directly the behaviour of the jet.

* Correspondence to: Institut de Mécanique des Fluides de Toulouse, UMR CNRS/INPT/UPST No. 5502, Avenue Camille Soula, 31400 Toulouse, France.
[1] E-mail: mohamedali.knani@ipeit.rnu.tn
[2] E-mail: taieb.lili@fst.rnu.tn
[3] E-mail: boisson@imft.fr

Received May 1999
Revised September 1999

As instability is the main concern of this work it should be remembered that according to Huerre and Monkewitz [6] plane shear layer instability occurs at the exhaust of the jet and dominates the potential core external flow.

The frequency of the developing vortices is then directly related to the most amplified mode of instability, first calculated by Michalke [7,8] and corresponding to a given Strouhal number based on the exhaust velocity of the jet and the momentum thickness of the outgoing initial shear layer.

Linear analysis theory indicates that the plane shear layer and thus the plane jet can be classified as convective instabilities (Huerre and Monkewitz [9], Ho and Huerre [10], Yu and Monkewitz [11]). That means that the amplified perturbations are convected downstream and the jet acts as an amplifier of initial flow perturbations. Absolute instabilities occurring in wakes or variable density jets are resonant modes and are observed whatever be the excitations. However, the case of spatially evolving shear layers and jets is in fact different from both these theoretical instabilities as a feedback mechanism is observed giving rise to stable mode response. This can be qualified as global instability and is the situation that is examined in this paper.

The present study aims to use an incompressible numerical simulation in order to determine the Reynolds number effect on the initial region of a near jet. For reasons that will be discussed further, the Reynolds numbers investigated ranged from 100 to 900. In this case viscous effects can be analysed. We will compare both forced and unforced jet in order to identify clearly the instability mechanism with respect to the specific length scales of the jet. Developing vortices are observed and their interactions by pairing are a function of these previous scales.

In this work different types of excitation are tested but the stress is put on a monochromatic excitation applied to the exhaust velocity used to stabilize the developing vortices. Results of these computations can be compared with other studies of the same type (Hussain and Thompson [2], Hsiao and Huang [12], Faghani *et al.* [13,14]). However, this paper addresses directly quite low Reynolds numbers not examined in these experimental papers. Many recent attempts have been conducted in round jets using direct numerical simulation or large eddy simulation that show the occurrence of low-order instability modes monitoring the development of the near jet region. Among these works we refer more precisely to the simulation of Danaila *et al.* [15] dealing with low-Reynolds number flows, a situation comparable with the one treated in the present paper. These authors have detailed the dynamics of these low-order modes in an unforced jet. Afterwards, their work was extended to combined excitations in order to provoke the complex situation of a bifurcating jet [16], a clear example of flow control by external excitation. The aim of the present paper is to focus on the effect of an excitation close to a naturally amplified mode. This constitutes a basis for further manipulation in more complex situations.

In the following we present successively the physical problem and boundary conditions (Section 2), the numerical method (Section 3), the transient to steady flow (Section 4), the flow excited by Dirac impulse excitation (Section 5) and the flow excited by sinusoidal oscillation (Section 6).

2. THE PHYSICAL PROBLEM

The domain of study is the plane jet issued from a wall and exhausting in an infinite domain filled with the same fluid. The flow is incompressible isothermal and considered as two-dimensional. This corresponds to the conditions that have been found by Faghani *et al.* [13] and Meyer *et al.* [17] in an experimental study at moderate Reynolds numbers. Moreover, as these authors and others have pointed out, the fact that varicose mode is more often observed for uniform flat velocity profiles at exhaust, the study is restricted to such perturbations and admits axial two-dimensional symmetry. Thus, half a domain is taken for the numerical simulation. Many tests have shown that this situation occurs naturally as far as the initial perturbation does not trend to force antisymmetrical sinuous mode. The flow pattern observed as a result of this model is not supposed to exist if the full jet is submitted to arbitrary perturbations as a competition with the sinuous mode may be at the disadvantage of the varicose mode. However, a monochromatic symmetrical excitation must produce this pattern as linear stability theory shows that this mode is amplified [18] in a plane jet. Danaila *et al.* [15] have observed similar varicose behaviour for round jets in the same Reynolds number range.

The domain is represented in Figure 1. The lateral extent of the domain is the width D containing the wall and the jet exhaust aperture H. The total length L of the domain is in the longitudinal direction. The geometry of the jet is such that L/H is constant and equal to 20, but the extent of the jet D/H is adapted to the lateral extent of the jet and varies with Reynolds number (see Table I).

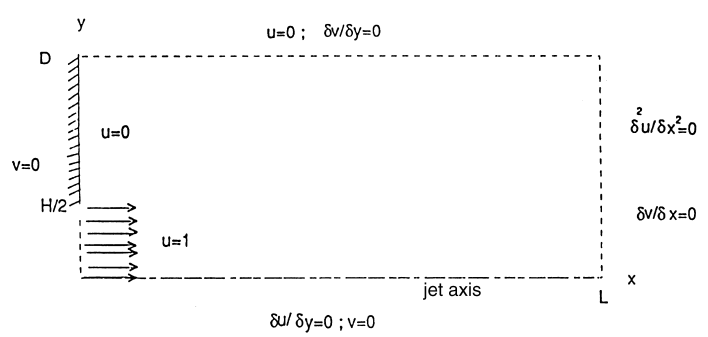

Figure 1. Domain and boundary conditions ($L/H = 20$; $H = 1$; $D/H = 3$ or 6).

Table I. Characteristic parameters of the simulation.

Re	100	300	500	700	900
D/H	6	3	3	3	3
T_0	180	150	120	150	180

Re, Reynolds number; D/H, width of the domain; T_0, duration of the initial computation.

One of the major problems in jet flow computation is the infinite domain and the free boundary conditions to impose in order to properly take account of this situation. The choice was crucial here and many tests have been done comparing three main types of outflow boundary conditions on the longitudinal velocity: (1) Neumann conditions; (2) convective boundary conditions; and (3) linear extrapolation of inside velocities (or zero second-order partial derivative of the U velocity at exit). None of them is purely satisfying but with respect to the discrete scheme used, the last one has been preferred. It corresponds to the choice made by Meyer *et al.* [1] and Estivalezes *et al.* [19].

For the entrainment boundary, the Neumann boundary condition is taken for the lateral velocity while keeping the longitudinal one at zero. Although rough, this condition seems to allow a sufficient freedom to the incoming flow as far as the corresponding frontier is put sufficiently far from the active vortical part of the jet. For the pressure it seems rather convenient to fix a single value in one position of the domain. The upper left corner provides the best stabilization of the solution. This choice is the empirical result of some preliminary tests. It cannot be considered as an absolute necessity but it fits better to the initial and boundary conditions for the coupled problem in our particular case.

3. NUMERICAL METHOD

The classical finite volume method [20] has been chosen to discretize the problem. The pressure implicit split operator (PISO) method derived by Issa [21] has been used to solve the incompressible flow problem ensuring exact mass conservation at each time step. The time step was maintained sufficiently small to catch the transient behaviour of the flow. A two-corrector step process is retained in accordance with the theoretical study on stability made by Issa [21]. As this method is widely described, we do not judge it necessary to reproduce its exact derivation and the corresponding operations. Interested readers are referred to Meyer *et al.* [1], Estivalezes *et al.* [19] and Hannoun *et al.* [22].

In the following, staggered uniform grids are chosen for lateral, longitudinal velocities and scalar properties (pressure). The time derivatives are Euler implicit and the space ones are second-order centred. This choice was made in accordance with the results of Meyer *et al.* [1], who tested this approach by comparison with experiments at a Reynolds number of 1700 and found reasonable agreement. As the viscous effect is more pronounced in the present work, the centred scheme will be even more adapted.

For these simulations we are interested in the near zone of the jet and this was limited to a length $L = 20H$. It was found that a value of $D = 3H$ is acceptable for all input Reynolds number greater or equal to 300. However, this size of the domain is not sufficient for lower Reynolds numbers. It was then necessary to double the width to $6H$. For comparison purposes we kept the mesh size constant at $\Delta x = 0.196$ and $\Delta y = 0.107$, which corresponds to meshes numbers of 102×28 and 102×56 for each class of Reynolds numbers (respectively greater (or equal to) and lower (or equal to) than 300). The mesh independence is difficult to verify in this simulation because reducing the spacing between points will also modify the initial shear layer thickness at the entrance that has been shown to be the main parameter for determining the frequency of the instability [1]. This has been checked by comparison of computation results

between two different meshes at a Reynolds number of 500. A finer grid of 153×42 with meshes reduced by a factor of 2/3 provides results that are displayed in Figures 2 and 3. The agreement is considered to be reasonably fair owing to the difference observed on the frequency of the instability. It has been also checked that after a transient regime the steady state velocity profiles are not affected when the grid is finer. The time step dictated by accuracy reasons was put to 10^{-2} s and the simulation duration is given in Table I. Note that duration T_0 is chosen in order to obtain a steady state after the first transient stage. A minimum value of T_0 is retained for $Re = 500$ in accordance with the results presented in Section 4. The convergence level for the continuity equation was fixed to 10^{-9}, a condition that maintains the number of internal iterations for linear systems solutions to a high value. This level of accuracy was imposed to avoid errors on the mass balance that could have an effect on the onset of instability. Tests have been performed to fix this level in order to maintain a reasonable computational effort. For solving these systems, the modified strongly implicit (MSI) method by Schneider and Zeddan [23] was used.

4. TRANSIENT AND STEADY STATE FLOW REGIME

For the first part of this work, the initial longitudinal velocity profile of the jet was maintained to a uniform value of 1 in the core region and 0 on the wall. The lateral velocity on the

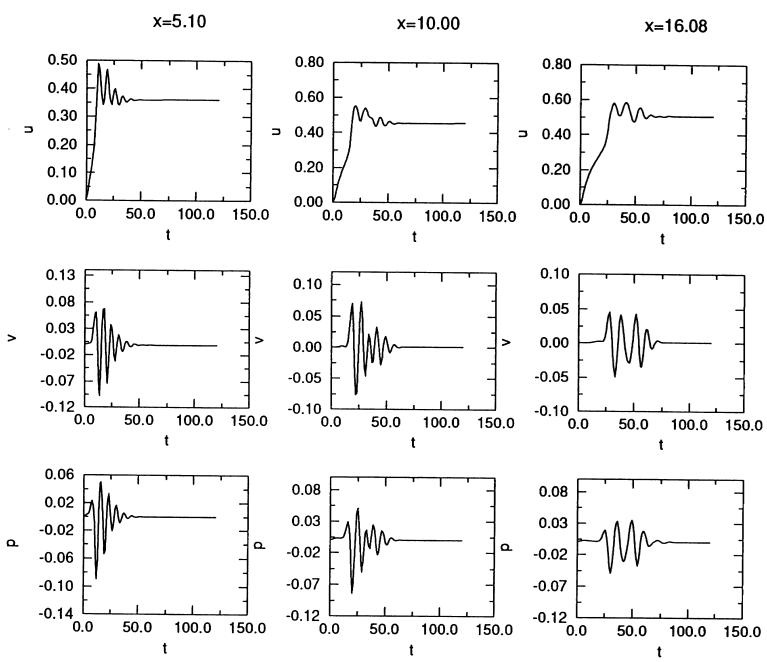

Figure 2. Time traces of velocity components and pressure at different longitudinal stations of the jet for a fixed lateral position ($y = 0.7$; $Re = 500$; non-excited jet; grid 102×28).

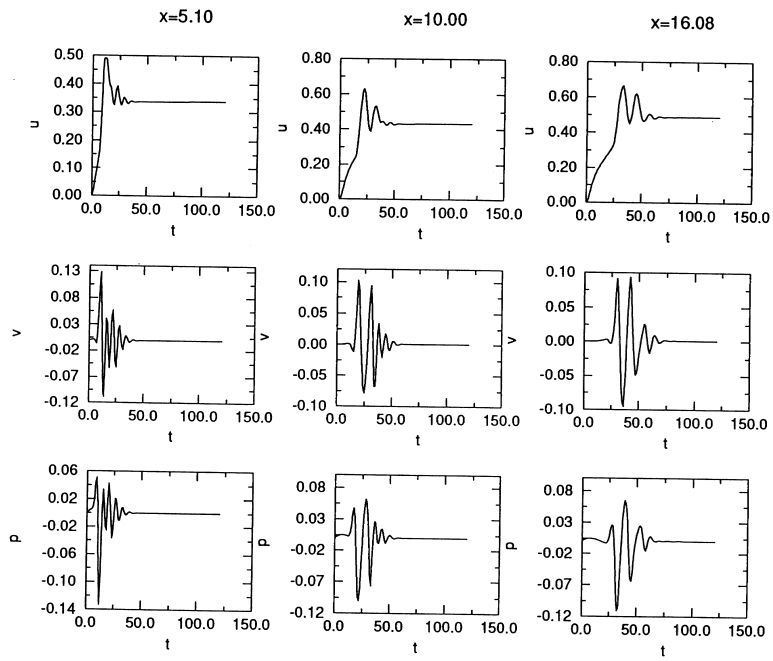

Figure 3. Same signals as in Figure 2 with a finer grid ($y = 0.7$; $Re = 500$; non-excited jet; grid 153×42).

entrance boundary is also equal to zero. The mesh size is kept constant. This provides similar conditions for all tests. Thus, the only parameter tuned when varying the Reynolds number is the kinematic viscosity of the fluid.

The computations all started from an arbitrary steady state corresponding to an inviscid jet $\{U_0 = 1$ for $0 < y < H/2$, $U_0 = V_0 = 0$ elsewhere for all x positions$\}$. At the first step of computation viscosity is added abruptly and introduces an artificial unphysical flow perturbation, even in a short period of time.

As a result of this perturbation, it is observed that a transient phenomenon takes place and some signals corresponding to the development of a vortex train are presented in Figure 2 for $Re = 500$. The same is also displayed in Figure 3 for a finer mesh that exhibits the same behaviour at a slightly different frequency. It should be noticed that this is but an example of what can be observed at other Reynolds number.

The interesting feature of this transient state is that after some time the oscillations die out and give rise to a steady state solution. For $Re = 500$ one can appreciate that this state is nearly reached after about 90 s and that it remains stable during the computation. In the figure, a period of 120 s is shown but no evolution was noticed while continuing the computation during another equivalent period of 120 s.

This period for stabilizing the flow is a function of the Reynolds number. If increased up to 900 a longer stabilization period is required because an increasing number of periods are

observed but the corresponding period of each is shorter. At $Re = 900$ the phenomenon seems to turn out to a pseudo periodic one and the steady state is not reached in the observation time. On the other hand, for smaller Reynolds numbers, the period enlarges requiring also a longer observation time but the number of events is smaller and turns to a single main oscillation and very small subsequent ones.

Nevertheless, after the stabilization period a steady state flow is observed and the longitudinal velocity profiles are presented in Figure 4 for the last time station of the corresponding computation. These Figures show that all profiles cross at a lateral distance close to 0.66 for all Reynolds number but the overall width of the profiles enlarges with Reynolds number. This signifies that the rate of growth of the jet is affected by an increasing viscous effect when the Reynolds number decreases. For $Re = 100$, the values inside the domain which are different to

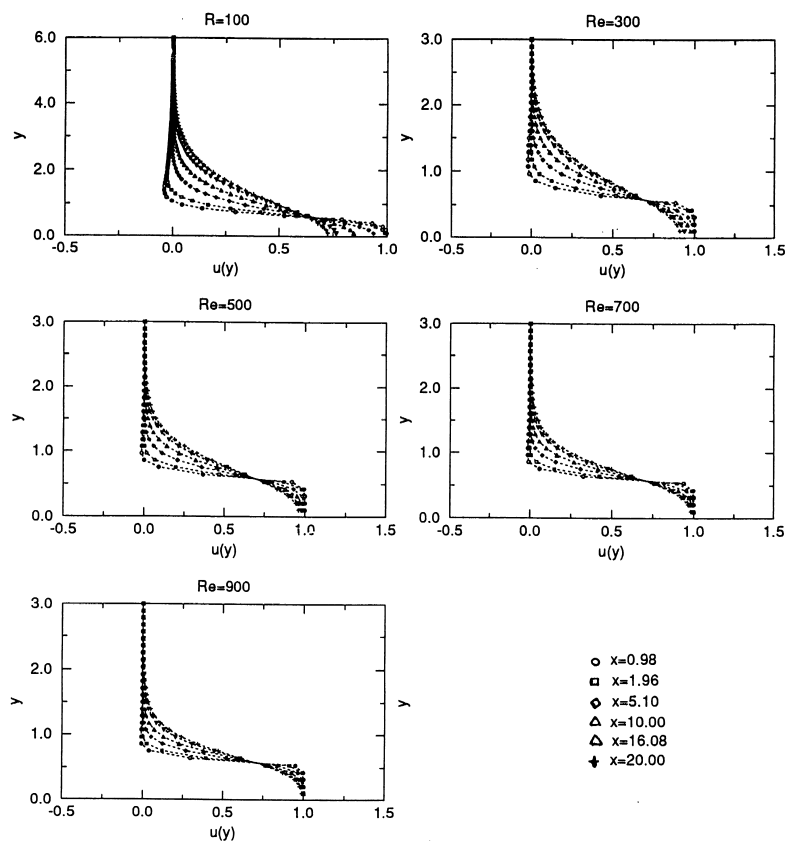

Figure 4. Longitudinal velocity profiles at different x stations (for the steady state at $t = 120$, 150 or 180 s; non-excited jet).

zero reach $y/D = 4$ and this clearly shows the reason for increasing the initial domain ($y/D = 3$). For this same case the velocity profile quickly turns to an approximately parabolic one in the core of the jet and return-flow is observed in the first sections of the jet.

Global parameters resulting from the evolution of the jet are presented in Figure 5. The frequency of instability in the transient stage (Figure 5(a)) exhibits a nearly linear increase with the Reynolds number. Similarly, the growth rate of the jet (Figure 5(b)) can be deduced from the value of b, the conventional width of the jet corresponding to $U = 0.5U_0$. It decreases with the Reynolds number but the decrease is much more important for the lowest values (500–100)

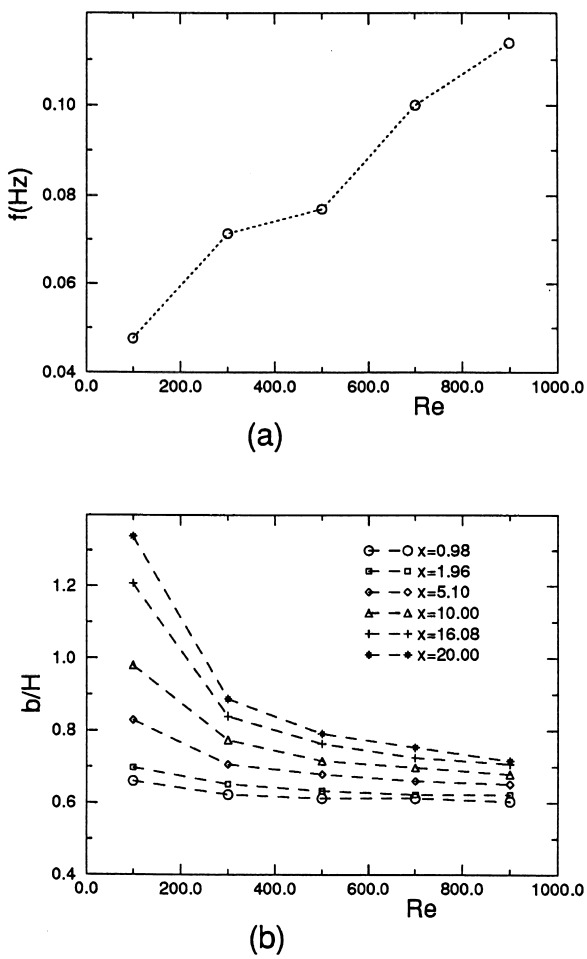

Figure 5. Frequency of vortex crossing (a) and width of the jet at different x stations (b) versus Reynolds number (non-excited jet).

than for the highest ones (900–500). At higher Reynolds numbers it has been found that the initial momentum thickness of the entrance velocity profile dominates the instability behaviour. The corresponding wavelength of shed vortices is such that pairing sequences occur in the shear layer around the potential core. In this simulation the vortices in the shear layer are of the order of the width of the jet entrance or even larger. The potential core is considerably shorter if it exists. The interaction with the jet column mode is direct. Thus, the width of the shear layer increases continuously with the Reynolds number and produces the vortex that is convected downstream.

The conclusion of this first part is that the code converges to a steady state flow configuration smearing out the effect of the transient. However, the behaviour of the transient is clearly linked to the Reynolds number. In the sequel, controlled perturbations will be imposed to this steady state in order to study the non-linear instability around this state.

5. TRANSIENT FLOW EXCITED BY A DIRAC IMPULSE

An arbitrary perturbation of the flow is first imposed on the form of a sudden impulse of the initial velocity profile. The impulse intensity is fixed to $5U_0$ for a single time step of 10^{-2} s.

$$\begin{cases} t = 0 & \vec{V}(x, y, t = 0) = \vec{V}(x, y, T_0) \quad 0 \le x \le L;\ 0 \le y \le D \\ t = 0.01 & U_e(t) = 5U_0 \qquad\qquad\qquad\quad x = 0;\ 0 \le y \le \dfrac{H}{2} \\ t > 0.01 & U_e(t) = U_0 \qquad\qquad\qquad\quad x = 0;\ 0 \le y \le \dfrac{H}{2} \end{cases}$$

where $\vec{V}(x, y, T_0)$ is the initial condition for the steady state obtained at $t = T_0$ for the velocity field and $U_e(t)$ is the boundary condition.

Velocity and pressure signals are displayed in Figure 6 for a Reynolds number of 500. It follows that the flow is submitted to an oscillating period and returns to the previous steady state as in the previous case. This is typically the behaviour of a convective instability. Note that the same number of crossing vortices is observed. Moreover, it can be found that the frequency and the duration of these oscillations are nearly independent of the amplitude and the duration of the pulse. The test has been made with an amplitude of $1.5U_0$ on a pulse of 5×10^{-2} s. The same frequency and the same number of vortices as in the simulation starting from zero are found.

These results show that the response of the jet in the near region is an intrinsic behaviour that selects the most amplified mode. The return to the same stable situation can indicate that the basic situation is well defined and that the results are quite independent of the impulse provided that the amplitude and the width of the pulse remain to be reasonably small values.

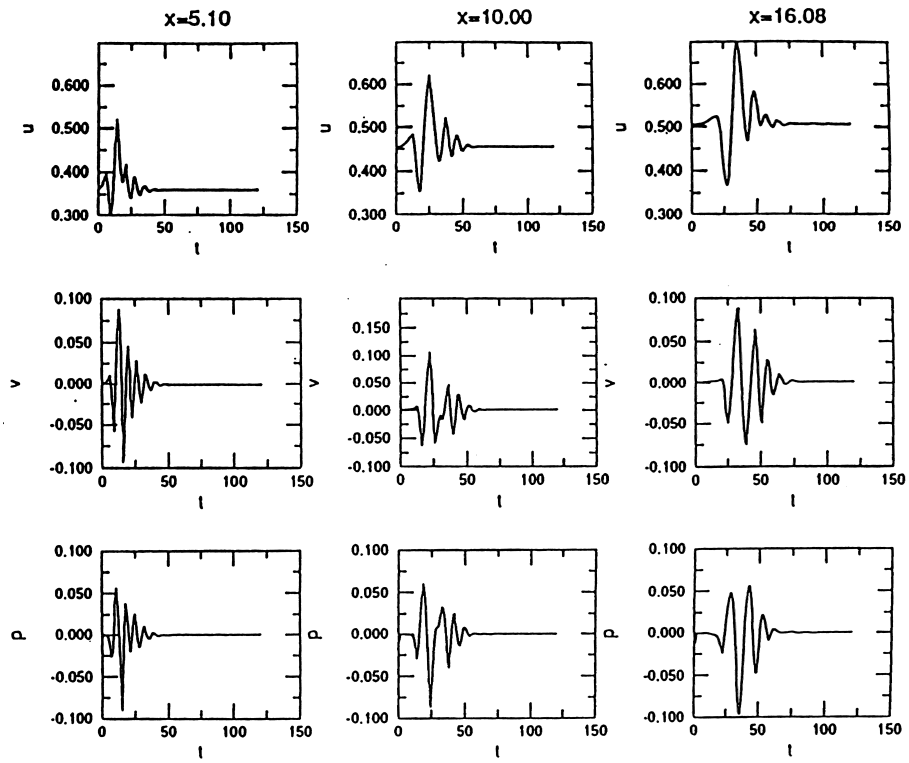

Figure 6. Time traces of velocity components and pressure at different longitudinal stations of the jet for a fixed lateral position ($y = 0.70$; $Re = 500$) (jet excited by impulse).

6. FLOW SUBMITTED TO SINUSOIDAL EXCITATION

A sinusoidal excitation is applied to the entrance velocity profile in order to stabilize the production of organized vortices. The following forced profile is imposed and maintained throughout the simulation:

$$\begin{cases} t = 0 \quad \vec{V}(x, y, t = 0) = \vec{V}(x, y, T_0) \quad 0 \le x \le L;\ 0 \le y \le D \\ t > 0 \quad U_e(t) = U_0[1 + \beta \sin(2\pi f_i t)] \quad x = 0;\ 0 \le y \le \dfrac{H}{2} \end{cases}$$

where β is the amplitude of the excitation and f_i is the forcing frequency.

The value of β was fixed to 0.025 and f_i to the previously observed natural frequency for each Reynolds number. Some preliminary tests have shown that an amplitude of 0.025 provides the best response compared with other different values (ranging from 10^{-2} to

2×10^{1}). The selected frequency f_i corresponds to the optimal receptivity of the incoming flow to the forcing. Many experimentalists have used the same technique to obtain regular vortex production and phase locking for the natural excitation frequency of the jet (Ho and Huang [24], Husain and Hussain [25], Faghani *et al.* [13] among others).

The signals obtained for $Re = 500$ are shown on Figure 7. It is clear that a periodic behaviour of the jet is observed; a situation that was expected at the view of the previously cited studies. It should be noticed that this monochromatic excitation at the natural frequency does not give rise to pairing phenomena on the studied domain.

The periodicity of the results infers also that the velocity flow is not perturbed by spurious reflections from the outflow boundary.

The iso-vorticity plots are given in Figure 8 in order to demonstrate the spatial structure of the flow at a Reynolds number of 500. The simulation starts with the steady flow and represents duration of 120 s that is to say approximately nine periods. Four different phases of the motion are caught from $t = 80$ to 110 s.

The wavelength of the vortical structures is such that two events can be clearly identified and the shed vortex leaves the domain quite smoothly. The lateral expansion of the jet imposes a corresponding growth of the travelling vortex but as mentioned before pairing is not observed to the contrary of what was found by Faghani *et al.* [13] for higher Reynolds numbers.

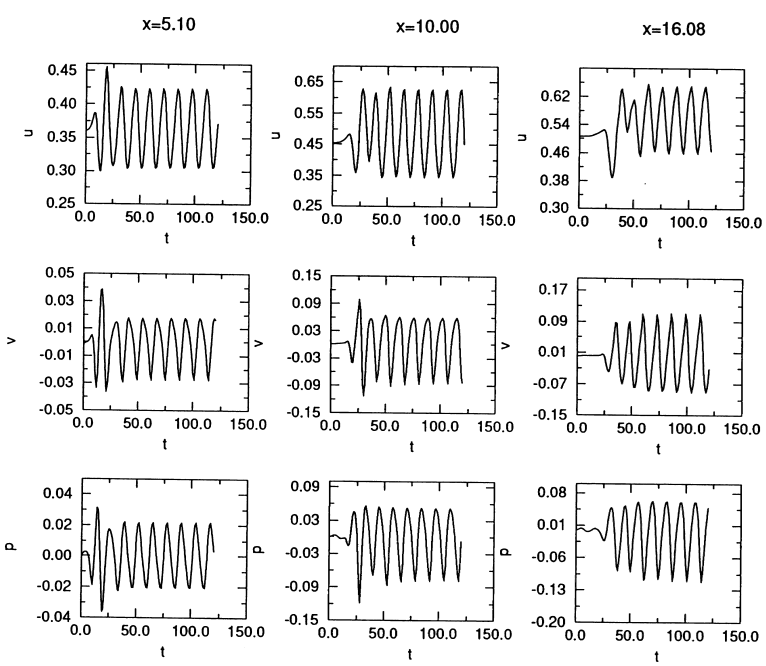

Figure 7. Time traces of velocity components and pressure at different longitudinal stations of the jet for a fixed lateral position ($y = 0.70$; $Re = 500$) (jet submitted to sinusoidal excitation: $\beta = 0.025$, $f_i = 0.077$).

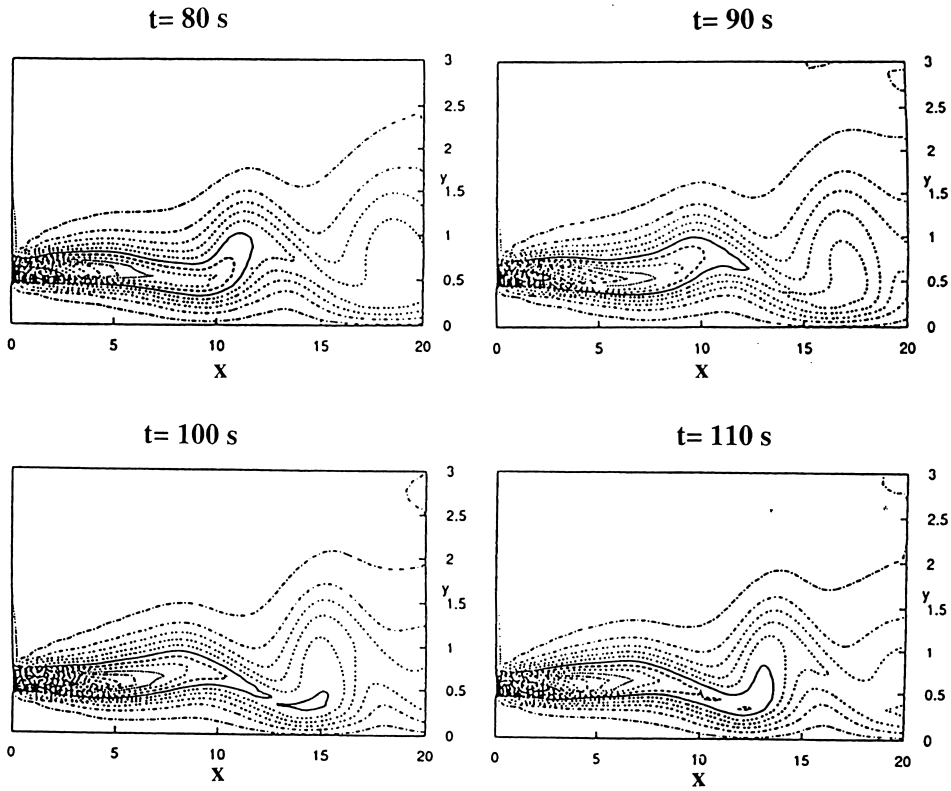

Figure 8. Iso-vorticity contours at $Re = 500$ for different time stations (jet submitted to sinusoidal excitation: $\beta = 0.025$, $f_i = 0.077$).

7. CONCLUSION

The results of this numerical simulation are used to point out the effect of Reynolds number on the development of instabilities in the near region of a plane jet. They correspond to a range where the convection is dominant near the axis but the viscous effect is not negligible in the vortex development.

A fairly simple method is used assuming that the flow is incompressible and the viscosity is strong enough to prevent from violent effects of partially reflective boundary conditions. The existence of a final steady state for the computation with constant input velocity seems to give some credibility to these assumptions.

The fact that this convergence is obtained allows us to examine the response of this flow to prescribed perturbations performing quite independently from the purely numerical perturbations due to the mismatching of initial conditions with the Navier–Stokes solution at the beginning of the first stage of computations.

The analysis of the response to a sudden impulse which is known to provide a broad band excitation have shown that the flow acts as an oscillator at the natural frequency that appeared first in the initial transient stage. This trends to confirm the intrinsic nature of the modal response of the jet.

On the basis of this analysis we have derived the preferred modes for the initial region of the jet and applied a forced excitation at this frequency in order to study the spatial development of the flow. This exercise turns out to be fruitful giving precise information on the parameters of the vortex generation attached to this instability mode.

These simulations tell us that the natural frequency of a jet can be tuned up at quite low Reynolds numbers and the time and length scales attached to this instability depends significantly on the viscosity of the flow.

It should be interesting for flow control operations that these parameters could be taken into account. In some particular low-velocity transport processes, unwanted oscillations can provide spurious instabilities and, in some others, prescribed forcing can help for installing controlled quasi-laminar mixing and transfer enhancement.

ACKNOWLEDGMENTS

The authors wish to thank the Director for International Relations of CNRS, the French Ministry of Foreign Affairs and the General Director of Scientific Research (DGRST) of Tunisia for financial support to this collaboration between the laboratories of both countries.

APPENDIX A. NOMENCLATURE

b	half-velocity width of the jet (for $U/U_a = 0.5$)
D	width of the domain
f	frequency
f_i	forcing frequency
H	width of the jet ($= 1$)
L	length of the domain
p	pressure
Re	Reynolds number ($U_0 H/v$)
t	current time
T_0	duration of the initial computation
U	longitudinal component of velocity
U_0	initial longitudinal velocity ($= 1$)
U_a	axial velocity
U_e	entrance velocity
V	lateral component of velocity
$\vec{V}(x, y, t)$	velocity field
x, y	space co-ordinates

Greek letters

β	amplitude of the excitation

$\delta/\delta x$	numerical partial derivatives
v	kinematic viscosity ($=1/Re$)

REFERENCES

1. Meyer J, Sévrain A, Boisson HC, Ha Minh H. Numerical simulation of a plane jet. In *Notes on Numerical Fluid Mechanics*, vol. 29, Wesseling P (ed.). Vieweg Verlag: Braunschweig, 1990; 363–371.
2. Hussain AKMF, Thompson CA. Controlled symmetric perturbation of the plane jet: an experimental study in the initial region. *Journal of Fluid Mechanics* 1980; **100**: 397–431.
3. Thomas FO, Goldschmidt VW. The possibility of a resonance mechanism in the developing two-dimensional jet. *Physics of Fluids* 1985; **28**(12): 3510–3514.
4. Sato H. The stability and transition of a two-dimensional jet. *Journal of Fluid Mechanics* 1960; **7**: 53–80.
5. Tatsumi T, Kakutani T. The stability of a two-dimensional laminar jet. *Journal of Fluid Mechanics* 1958; **4**: 261–275.
6. Huerre P, Monkewitz PA. Local and global instability in spatially developing flows. *Annual Review of Fluid Mechanics* 1990; **22**: 473–537.
7. Michalke A. On the inviscid instability of the hyperbolic tangent velocity profile. *Journal of Fluid Mechanics* 1964; **16**: 543–556.
8. Michalke A. On spatially growing disturbances in an inviscid shear layer. *Journal of Fluid Mechanics* 1965; **23**: 521–544.
9. Huerre P, Monkewitz PA. Absolute and convective instabilities in free shear layers. *Journal of Fluid Mechanics* 1985; **159**: 151–168.
10. Ho ChM, Huerre P. Perturbed free shear layers. *Annual Review of Fluid Mechanics* 1984; **16**: 365–424.
11. Yu MH, Monkewitz PA. Oscillations in the near field of a heated two-dimensional jet. *Journal of Fluid Mechanics* 1993; **255**: 323–347.
12. Hsiao FB, Huang JM. On the evolution of instabilities in the near field of a plane jet. *Physics of Fluids* 1990; **A2**(3): 400–412.
13. Faghani D, Sevrain A, Boisson HC. Vortical structure of an acoustically forced plane jet: bi-orthogonal eddies vs. physical eddies. In *Proceedings of the 11th Symposium on Turbulent Shear Flows*, Grenoble, 8–10 September, vol. 2, Binder G (ed.). Institut National Polytechnique de Grenoble, 1997; 22.7–22.11.
14. Faghani D, Sévrain A, Boisson HC. Physical eddy recovery through bi-orthogonal decomposition in an acoustically forced plane jet. *Flow Turbulence and Combustion* 1999; **62**: 69–88.
15. Danaila I, Dusek J, Anselmet F. Coherent structures in a round, spatially evolving, unforced, homogeneous jet at low Reynolds numbers. *Physics of Fluids* 1997; **9**(11): 3323–3342.
16. Danaila I, Boersma BJ. Direct numerical simulation of bifurcating jets. *Physics of Fluids* 2000; **12**(5): 1255–1257.
17. Meyer J, Sevrain A, Boisson HC, Ha Minh H. Organized structures and transition in the near field of a plane jet. In *Structure of Turbulence and Drag Reduction*, IUTAM Symposium, Zurich, Switzerland 1989, Gyr A (ed.). Springer: Berlin, 1990.
18. Variéras D. Etude de l'écoulement et du transfert de chaleur en situation de jet plan confiné. PhD thesis, Université Paul Sabatier, Toulouse, No. 3632, 2000.
19. Estivalèzes JL, Boisson HC, Kourta A, Chassaing P, Ha Minh H. An implicit pressure–velocity algorithm applied to oscillatory convection in low Prandtl fluid. In *Numerical Simulation of Oscillatory Convection in Low Pr Fluids*, *Notes on Numerical Fluid Mechanics*, vol. 27, Roux B (ed.). Vieweg Verlag: Heidelberg, 1989; 128–135.
20. Patankar SV. *Numerical Heat Transfer and Fluid Flow*. Hemisphere Publishing Corporation: New York, 1980.
21. Issa RI. Solution of the implicitly discretised fluid flow equations by operator-splitting. *Journal of Computational Physics* 1986; **62**(1): 40–65.
22. Hannoun N, Boisson HC, Ben Abdesselam A. Open boundary conditions for an implicit compressible Navier–Stokes solver. *8eme Journées Internationales de Thermique*, *Marseille* 1997; **2**: 47–54.
23. Schneider GE, Zedan M. A modified strongly implicit procedure for the numerical solution of field problems. *Numerical Heat Transfer* 1981; **4**: 1–19.
24. Ho ChM, Huang LS. Subharmonics and vortex merging in mixing layers. *Journal of Fluid Mechanics* 1982; **119**: 443–473.
25. Husain HS, Hussain F. Experiments on subharmonic resonance in shear layer. *Journal of Fluid Mechanics* 1995; **304**: 343–372.

